

ROBUST SPARSE HYPERSPECTRAL UNMIXING BASED ON MULTI-OBJECTIVE OPTIMIZATION

Xia Xu¹, Liming Wang², Bin Pan¹ and Zhenwei Shi¹

¹Image Processing Center, School of Astronautics, Beihang University, Beijing 100191, China

²State Key Laboratory of Information Security, Institute of Information Engineering Chinese Academy of Sciences, Beijing 100093, China
{xuxia,panbin,shizhenwei}@buaa.edu.cn

ABSTRACT

Sparse representation based hyperspectral unmixing methods have attracted increasing investigations during the past decade. Recently, multiple signal classification (MUSIC) algorithm has been verified effective in reducing the mutual coherence of the spectral library. However, the popular pre-pruning strategy by MUSIC cannot guarantee that the endmembers exactly exist in the selected spectral subset when the image noise is serious. In this paper, we propose a new sparse unmixing method for hyperspectral images via integrating the pruning operation into the optimization process. The projection of the library is represented by an objective function in the proposed method. To avoid the manually settings of regularization parameters, we develop a new multi-objective based method where reconstruction error, sparsity error and the projection function are considered as three parallel objectives that could be optimized simultaneously. Experimental results have indicated the superiority of the proposed method, especially in high-noise conditions.

Index Terms— Sparse unmixing, multi-objective optimization, hyperspectral images

1. INTRODUCTION

Pixels in hyperspectral images (HSIs) are often mixed due to the low spatial resolution. The process of recovering pure materials (endmembers) and estimating their proportions (abundances) is called unmixing [1]. Recently proposed unmixing methods mainly include geometry, statistics and sparse based [1]. Among them sparse unmixing attracts increasing attention since there is no need to assume the existence of pure pixels in the image [2–7].

This paper is inspired by the work MUSIC-CSR (multiple signal classification and collaborative sparse regression) pro-

posed in [6]. In MUSIC-CSR, the authors used the multiple signal classification (MUSIC) algorithm to prune the spectral library and then performed the classic sparse unmixing method. This method can be considered as a framework, where MUSIC could be used as a pre-pruning operation. The work in [6] has shown that MUSIC could significantly improve the unmixing performance.

However, there are some limitations in [6]. First, this algorithm include two-steps: pre-pruning and unmixing. The authors theoretically proved that endmembers will exist in the selected spectral subset by MUSIC if there is no noise. However, due to the unavoidable noise in the image, it is hard to guarantee that endmembers are exactly included in the subset. The situation becomes even worse when the noisy is strong. Overall, the preprocessing strategy of library pruning is difficult to avoid the loss of information.

In this paper, we consider incorporating MUSIC as an objective function into the sparse unmixing framework. An intuitive idea is to add it as a new regularization term. However, there are two difficulties in this case. Firstly, optimization variable of sparse unmixing is the abundances, while MUSIC aims to prune the spectral library. Secondly, even though the regularizer is added, two regularization coefficients have to be manually adjusted, which would reduce the robustness of the unmixing method.

In order to overcome the above two problems, we propose a multi-objective optimization (MO) [8, 9] based sparse unmixing algorithm (MUSIC-MoSU), where reconstruction error, sparsity errors and projection are taken as three objective functions. The endmember selection and library pruning are integrated into a unified framework, and nonnegative least squares are used to inverse the abundances. The major novelties of MUSIC-MoSU include three aspects: optimization objectives, optimization method and parameter adjustment.

- The pruning operation is taken as one of the objective functions into the optimization process. The main difference between MUSIC-MoSU and MUSIC-CSR is that the search space of MUSIC-MoSU is gradually compressed, while MUSIC-CSR directly compresses

Thanks to the National Key R&D Program of China under the Grant 2017YFC1405600, National Natural Science Foundation of China under the Grants 61671037, and the Excellence Foundation of BUAA for PhD Students under Grant 2017057. *Corresponding author: Liming Wang (wangliming@iie.ac.cn) and Zhenwei Shi.*

the search space into a smaller subset where the final unmixing result depends on the correctness of the subset.

- In order to make the proposed method feasible to solve, we transform the endmember selection problem into a binary sparse problem. In MUSIC-MoSU, the spectral library is represented by a binary vector, where locations corresponding to the selected endmembers are set as “1” and “0” otherwise. By this means the sparse unmixing has been transformed to an ℓ_0 -based optimization problem. This paper presents a multi-objective optimization method to solve it without any approximation, which is beneficial to find the global optimal solution.
- MUSIC-MoSU can avoid the adjustment of regularization coefficients. The three objective functions are optimized simultaneously. There is no need of regularization parameters to balance them, which is very helpful to improve the robustness of unmixing algorithms.

2. PROPOSED METHOD

2.1. Optimization problem

Although the MUSIC algorithm provides a pre-pruning for the library, the ℓ_1 norm based MUSIC-CSR could not obtain a sufficient sparse results. Moreover, MUSIC may prune some favorable spectra. Thus in this paper, MUSIC-MoSU is proposed to integrate the advantage of MUSIC into the optimization process of sparse unmixing, and balance it with the reconstruction error and sparsity error.

Let $\mathbf{Y} = [\mathbf{y}_1, \dots, \mathbf{y}_n] \in \mathbb{R}^{L \times n}$ be the measured hyperspectral data with L bands and n pixels, $\mathbf{A} = [\mathbf{a}_1, \dots, \mathbf{a}_m] \in \mathbb{R}^{L \times m}$ be the spectral library with m pure materials. The optimization problem of MUSIC-MoSU is

$$\begin{aligned} \min_{\mathbf{s} \in \{0,1\}^m} F(\mathbf{s}) &= [f_1(\mathbf{s}), f_2(\mathbf{s}), f_3(\mathbf{s})]^T \\ f_1(\mathbf{s}) &= \begin{cases} +\infty, & \|\mathbf{s}\|_1 = 0 \text{ or } \geq 2k \\ \|\mathbf{Y} - \mathbf{A}_s \mathbf{X}_s\|_F, & \text{otherwise} \end{cases} \\ f_2(\mathbf{s}) &= |\|\mathbf{s}\|_1 - k| \\ f_3(\mathbf{s}) &= \|\mathbf{P}_{\mathbf{A}_s}^\perp \mathbf{A}_s\|_F \end{aligned} \quad (1)$$

where $\mathbf{s} = [s_1, \dots, s_m]$ is a binary representation of the library \mathbf{A} , $\|\mathbf{s}\|_1$ denotes the endmember number represented by a certain individual, k is the actual number of endmembers, \mathbf{A}_s is the corresponding subset of spectral library, \mathbf{X}_s is the abundances of endmembers, $\mathbf{P}_{\mathbf{A}_s}^\perp$ is the projector on $\text{range}(\mathbf{A}_s)^\perp$, $f_1(\mathbf{s})$ is the reconstruction error function, $f_2(\mathbf{s})$ is the endmember sparsity error, $f_3(\mathbf{s})$ is the projection of \mathbf{A}_s . $f_1(\mathbf{s})$ is meaningful if $0 < \|\mathbf{s}\|_1 < 2k$ to exclude trivial or overly bad solutions. It is worth noticing that k is usually unknown in

practical application, so HySime method [10] is used to give it an estimation in this paper.

2.2. Concentration of individuals

MO aims at finding a set of evenly-distributed and non-dominated solutions to provide a balance for the objectives. However, a single solution is required for sparse unmixing. Thus in this paper, the MO framework of multi-objective evolutionary algorithm based on decomposition (MOEA/D) [11] is improved to solve the decision making problem. The improved subproblem is

$$\begin{aligned} \min_{\mathbf{s}} g^{te}(\mathbf{s}|\boldsymbol{\lambda}, \mathbf{z}^*) &= \max_{1 \leq i \leq 3} \{\lambda_i |f_i(\mathbf{s}) - z_i^*|\} \\ \text{s.t. } 0 < \|\mathbf{s}\|_1 < 2k \end{aligned} \quad (2)$$

where \mathbf{z}^* is the ideal point in current iteration with $\mathbf{z}^* = \min\{\|F_j(\mathbf{s})\|, j = 1, \dots, p\}$, p is the population size, $\boldsymbol{\lambda}$ is the weight vector with $\boldsymbol{\lambda} \geq 0$ and $\boldsymbol{\lambda}^T \mathbf{1} = 1$, λ_i is the weight of the i th objective, $g^{te}(\mathbf{s}|\boldsymbol{\lambda}, \mathbf{z}^*) = \max_{1 \leq i \leq 3} \{\lambda_i |f_i(\mathbf{s}) - z_i^*|\}$ is the weighted Tchebycheff distance of individual \mathbf{s} to the ideal point \mathbf{z}^* .

In original MOEA/D, the ideal point is defined as $\mathbf{z}_M^* = [z_1^*, z_2^*, z_3^*]^T$, $z_i^* = \min\{f_i(\mathbf{s}_1), \dots, f_i(\mathbf{s}_p)\}$. Fig. 1 shows the difference of ideal points in the original MOEA/D and MUSIC-MoSU. From Fig. 1, \mathbf{z}_M^* is a virtual point where all the objectives achieve minimums simultaneously. For the original MOEA/D, the problem of different $\boldsymbol{\lambda}$ could generate different optimal solution (dashed rectangular boxes in Fig. 1). Thus several non-dominated solutions could be obtained. However, the ideal point \mathbf{z}^* in MUSIC-MoSU is a real individual that has minimum distance to the original point. In this case, the individual that has minimum g^{te} to \mathbf{z}^* is itself. More and more individuals are replaced by the ideal point. Finally, the whole population is concentrated to a single solution.

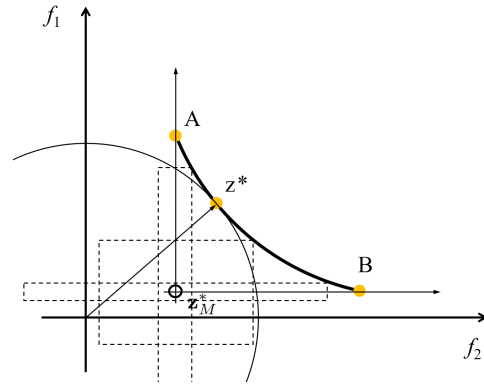


Fig. 1: An illustration about the difference of ideal points in the original MOEA/D and MUSIC-MoSU. \mathbf{z}_M^* is the ideal point in MOEA/D. \mathbf{z}^* is the ideal point in MUSIC-MoSU. \widehat{AB} is the Pareto optimal front.

2.3. Optimization Process

The optimization process of MUSIC-MoSU is shown in **Algorithm 1**. A population is initialized in the beginning. In the iteration process, for each individual \mathbf{s}_i , a new individual \mathbf{s}'_i is generated based on the bit-wise flipping strategy, where each location is flipped to its opposition with a probability $1/m$ (line 9). The ideal point \mathbf{z}^* is updated if the new individual is closer to the original point (line 11, 12). For the neighbours of \mathbf{s}_i , the individuals that are farther to the original point than \mathbf{s}'_i are replaced by \mathbf{s}'_i (line 12-14). After several iterations, the final solution \mathbf{s}^* of Eq. (1) is obtained and the corresponding spectra $\mathbf{A}_{\mathbf{s}^*}$ are endmembers (line 15). At last, nonnegative least squares is used to inverse the abundances of endmembers (line 17).

Algorithm 1: MUSIC-MoSU

Input: hyperspectral image data \mathbf{Y} , spectral library \mathbf{A} .
Output: abundance fractions \mathbf{X} .

- 1 **Preprocessing:**
- 2 Estimate the number of active endmembers as \hat{k} of the hyperspectral image using HySime.
- 3 **Initialization:**
- 4 population size p , maximum iteration number T , a population $\mathbf{S} = \{\mathbf{s}_1, \dots, \mathbf{s}_p\}$, a set of weight vector $\mathbf{\Lambda} = \{\boldsymbol{\lambda}_1, \dots, \boldsymbol{\lambda}_p\}$, each subproblem's neighbors $\{B_1, \dots, B_p\}$, the ideal point \mathbf{z}^* .
- 5 **Endmember Selection:**
- 6 **while** $t < T$ **do**
- 7 $t = t + 1$;
- 8 **for** $i = 1, \dots, p$ **do**
- 9 Generate a new individual \mathbf{s}'_i from \mathbf{s}_i based on bit-wise flipping strategy, where each location is flipped with a probability $1/m$;
- 10 **if** $\|F(\mathbf{s}^*)\|_2 > \|F(\mathbf{s}'_i)\|_2$ **then**
- 11 Set $\mathbf{z}^* = F(\mathbf{s}'_i)$
- 12 **for** $j \in B_i$ **do**
- 13 **if** $g_i^{te}(\mathbf{s}'_i | \boldsymbol{\lambda}_i, \mathbf{z}^*, \mathbf{s}^*) \leq g_j^{te}(\mathbf{s}_j | \boldsymbol{\lambda}_j, \mathbf{z}^*, \mathbf{s}^*)$ **then**
- 14 Set $\mathbf{s}_j = \mathbf{s}'_i$ and $F(\mathbf{s}_j) = F(\mathbf{s}'_i)$
- 15 Return the final solution as \mathbf{s}^* and record the corresponding spectral signatures.
- 16 **Abundance Estimation:**
- 17 Compute the abundances for the whole hyperspectral image based on nonnegative least squares algorithm:
 $\mathbf{X} = \arg \min_{\mathbf{X} \geq 0} \|\mathbf{Y} - \mathbf{A}_{\mathbf{s}^*} \mathbf{X}\|_F$

3. EXPERIMENTS

In this section, some experiments are conducted to test the performance of MUSIC-MoSU. Due to the fact that groundtruth of real-world hyperspectral images is hard to get, synthetic data are used in this paper. The synthetic data is generated based on the the United States Geological Survey (USGS) digital spectral library (splib06a)¹, which contains 498 spectra under 224 bands. 4 to 10 spectra are selected as

¹Available online: <http://speclab.cr.usgs.gov/spectral-lib.html>

endmembers respectively (i.e. $k=4$ to 10). Among them, five similar spectra: Actinolite HS116.3B, Actinolite HS22.3B, Actinolite HS315.4B, Actinolite NMNH80714 and Actinolite NMNHR16485 are selected specially to increase the data complexity. Each image in this dataset has a size of 64×64 and is corrupted by 20/30dB noise respectively.

Five recently proposed sparse unmixing algorithms, SUNSAL [2], SUNSAL-TV [3], SMP [5], RSFoBa-2, RSFoBa-Inf [4] and MUSIC-CSR [6] are taken for comparison. Because the proposed method is developed under the basis of MUSIC-CSR, the comparison with this algorithm should be paid special attention. Signal-to-reconstruction error ($SRE \equiv 10 \log_{10} \left(\frac{E[\|\mathbf{X}\|_F^2]}{E[\|\mathbf{X} - \hat{\mathbf{X}}\|_F^2]} \right)$) is used to evaluate their performance, where \mathbf{X} is the true abundances and $\hat{\mathbf{X}}$ is the estimation. For parameters setting, the default values in MOEA/D are taken and the maximum iteration number is set experientially.

Table 1 shows the SRE results of these algorithms. From the results, MUSIC-MoSU could surpasses the other six methods in most cases, especially when noise is stronger and k is larger. It is slightly worse than RSFoBa-Inf when $k = 5$ and $k = 6$ in 20dB noise cases. All results of MUSIC-MoSU are better than MUSIC-CSR. In fact, the endmembers obtained by MUSIC-MoSU cover the real ones in all the cases. When the noise is 20dB, MUSIC-MoSU could find a little more endmembers. When the noise is 30dB, MUSIC-MoSU could exactly obtain the real endmembers.

Results in Table 1 indicate that MUSIC-MoSU achieves better performance than MUSIC-CSR where pre-pruning strategy was adopted. This result is also the experimental validation for our theoretical analysis.

4. CONCLUSION

In this paper, a tri-objective optimization based sparse unmixing algorithm MUSIC-MoSU is proposed, where the reconstruction error, sparsity error and projection are considered as three parallel objectives. The projection objective takes the advantage of the MUSIC algorithm, and further integrates it into the unmixing optimization process. This improvement could avoid the information loss in the library pre-pruning strategy. Moreover, to solve the decision making problem in MO, MUSIC-MoSU improves the ideal point in MOEA/D to a real individual. Experiments on synthetic data have verified the effectiveness of MUSIC-MoSU. In the future extended journal paper, we will conduct more synthetic and real data experiments for comparison and parameters discussion.

5. REFERENCES

- [1] J. M. Bioucas-Dias, A. Plaza, N. Dobigeon, M. Parente, Q. Du, P. Gader, and J. Chanussot, "Hyperspectral unmixing overview: geometrical, statistical, and sparse

Table 1: SRE results of SUnSAL, SUnSAL-TV, SMP, RSFoBa-2, RSFoBa-Inf, MUSIC-CSR and MUSIC-MoSU on synthetic data.

SNR	k	SUnSAL	SUnSAL-TV	SMP	RSFoBa-2	RSFoBa-Inf	MUSIC-CSR	MUSIC-MoSU
20dB	4	3.2859	2.7133	2.5247	5.5936	7.2252	4.2356	8.9568
	5	3.0177	2.3333	3.1640	5.1796	7.4656	4.2412	5.8819
	6	3.3636	2.8785	5.7019	4.8328	6.8875	4.6673	5.4218
	7	3.2529	2.9369	4.0000	3.2330	4.0024	5.2210	7.3740
	8	2.3822	2.2278	3.9736	3.2649	3.1887	4.8399	8.1630
	9	2.7601	2.6670	3.8935	2.2126	3.2803	4.2761	7.2029
	10	3.1040	2.8547	4.7120	2.4319	2.3627	4.0438	7.8342
30dB	4	9.5467	7.2716	3.5312	15.5788	14.9340	13.2320	19.4240
	5	9.0219	6.6205	4.9450	11.4852	15.0515	13.0011	17.6580
	6	9.2247	6.9537	5.5319	12.1946	14.2658	12.9473	18.0181
	7	8.8378	7.0158	4.9014	11.1182	13.7916	12.0716	17.5835
	8	7.9069	6.5309	6.1130	11.0099	12.9609	11.6372	17.6047
	9	8.1637	6.8764	7.2575	11.4615	13.0453	12.0128	18.0314
	10	8.8004	7.4107	6.5900	10.7358	12.5587	11.9462	18.3527

regression-based approaches,” *IEEE Journal of Selected Topics in Applied Earth Observations and Remote Sensing*, vol. 5, no. 2, pp. 354–379, 2012.

- [2] J. M. Bioucas-Dias and M. A. T. Figueiredo, “Alternating direction algorithms for constrained sparse regression: Application to hyperspectral unmixing,” in *2nd Workshop on Hyperspectral Image and Signal Processing: Evolution in Remote Sensing, WHISPERS 2010*, 2010, pp. 1–4.
- [3] M. D. Iordache, J. M. Bioucas-Dias, and A. Plaza, “Total variation spatial regularization for sparse hyperspectral unmixing,” *IEEE Transactions on Geoscience and Remote Sensing*, vol. 50, no. 11, pp. 4484–4502, 2012.
- [4] W. Tang, Z. Shi, and Y. Wu, “Regularized simultaneous forward-backward greedy algorithm for sparse unmixing of hyperspectral data,” *IEEE Transactions on Geoscience and Remote Sensing*, vol. 52, no. 9, pp. 5271–5288, 2014.
- [5] Z. Shi, W. Tang, Z. Duren, and Z. Jiang, “Subspace matching pursuit for sparse unmixing of hyperspectral data,” *IEEE Transactions on Geoscience and Remote Sensing*, vol. 52, no. 6, pp. 3256–3274, 2014.
- [6] M. D. Iordache, J. M. Bioucas-Dias, A. Plaza, and B. Somers, “MUSIC-CSR: Hyperspectral unmixing via a multiple signal classification and collaborative sparse regression,” *IEEE Transactions on Geoscience and Remote Sensing*, vol. 52, no. 7, pp. 4364–4382, 2014.
- [7] R. Feng, Y. Zhong, and L. Zhang, “Adaptive spatial regularization sparse unmixing strategy based on joint MAP for hyperspectral remote sensing imagery,” *IEEE Journal of Selected Topics in Applied Earth Observations and Remote Sensing*, vol. 9, no. 12, pp. 5791–5805, 2016.
- [8] M. Gong, H. Li, E. Luo, J. Liu, and J. Liu, “A multi-objective cooperative coevolutionary algorithm for hyperspectral sparse unmixing,” *IEEE Transactions on Evolutionary Computation*, vol. 21, no. 2, pp. 234–248, 2017.
- [9] X. Xu and Z. Shi, “Multi-objective based spectral unmixing for hyperspectral images,” *ISPRS Journal of Photogrammetry and Remote Sensing*, vol. 124, pp. 54–69, 2017.
- [10] J. M. Bioucas-Dias and J. M. P. Nascimento, “Hyperspectral subspace identification,” *IEEE Transactions on Geoscience and Remote Sensing*, vol. 46, no. 8, pp. 2435–2445, 2008.
- [11] Q. Zhang and H. Li, “MOEA/D: A multiobjective evolutionary algorithm based on decomposition,” *IEEE Transactions on Evolutionary Computation*, vol. 11, no. 6, pp. 712–731, 2007.